Contributed papers

Synergistic effect of ethyl phosphonate and Zn^{2+} in low chloride media

Susai Rajendran
B.V. Apparao and
N. Palaniswamy

The authors

Susai Rajendran is with the Department of Chemistry, GTN Arts College (Autonomous), Dindigul, Tamilnadu, India.

B.V. Apparao is with the Department of Chemistry, Regional Engineering College, Warangal, Andhrapradesh, India.

N. Palaniswamy is with the Corrosion Science and Engineering Division, Central Electrochemical Research Institute, Karaikudi, Tamilnadu, India.

Abstract

The synergistic effect of sodium salt of ethyl phosphonic acid (EPA) and Zn^{2+} on the inhibition of corrosion of mild steel in neutral aqueous environment containing 60 ppm Cl^- has been evaluated by the weight-loss method. The formulation consisting of 300 ppm EPA and 300 ppm Zn^{2+} has 88 per cent inhibition efficiency. The nature of the protective film formed on the metal surface has been analysed by x-ray diffraction, FTIR, uv-visible and luminescence spectra. The protective film is found to be luminescent and to consist of Fe^{2+} –EPA complex, $Zn(OH)_2$ and a very thin film of oxides of iron.

Anti-Corrosion Methods and Materials
Volume 45 · Number 5 · 1998 · pp. 338–343

Several phosphonic acids have been used as corrosion inhibitors, due to their ability to form complexes with metal ions and scale inhibiting property[1-11]. The present work is undertaken:

- to study the synergistic effect of sodium salt of ethyl phosphonic acid (EPA) and Zn^{2+} on the inhibition of corrosion of mild steel in neutral aqueous environment containing 60ppm Cl^-, a situation commonly encountered in cooling water technology; and
- to understand the nature of the protective film by using x-ray diffraction, FTIR, uv-visible and luminescence spectra.

Experimental

Preparation of the specimens

Mild steel specimens (0.02-0.03 per cent S, 0.03-0.08 per cent P, 0.4-0.5 per cent Mn, 0.1-0.2 per cent C and the rest iron) of the dimensions $1 \times 4 \times 0.2$cm were polished to mirror finish and degreased with trichloroethylene and used for the weight-loss method and surface examination studies.

Weight-loss method

Three mild steel specimens were immersed in 100ml of the solutions containing various concentrations of the inhibitor in the absence and presence of Zn^{2+}, for a period of seven days. The weights of the specimens before and after immersion were determined using a Mettler balance, AE-240.

Surface examination study

The mild steel specimens were immersed in various test solutions for a period of two days. After two days, the specimens were taken out and dried. The nature of the film formed on the surface of the metal specimens was analysed by various surface analysis techniques.

S. Rajendran is thankful for the University Grants Commission, New Delhi, India, for awarding financial assistance, to the executive director, Sasha Industries Limited, Dindigul, and to Mr Ranjit Soundararajan, the correspondent, Professor S. Ramakrishnan, the principal and Professor P. Jayaram, the HOD of Chemistry Department, G.T.N. Arts College (Autonomous), Dindigul and to Mr A.A. Joseph and Er. Veluswamy, CECRI, Karaikudi for their help.

Anti-Corrosion Methods and Materials
Volume 45 · Number 5 · 1998 · 338–343

The FTIR spectra

The FTIR spectra were recorded using a Perkin-Elmer 1600 FTIR spectrophotometer.

The uv-visible spectra

The uv-visible reflectance spectra were recorded using a Hitachi U-3400 spectrophotometer. The same instrument was used for recording uv-visible absorption spectra of aqueous solutions also.

X-ray diffraction technique

The XRD patterns of the film formed on the metal surface were recorded using a computer controlled x-ray powder diffractometer, JEOL, JDX 8030 with CuKa(Ni-filtered) radiation (l = 1.5418 Å) at a rating of 40kV, 20mA.

Luminescence spectra

The luminescence spectra of the film formed on the metal surface were recorded using a Hitachi 650-10 S fluorescence spectrophotometer equipped with a 150W Xenon lamp and a Hamamatsu R 928 F photomultiplier tube. The emission spectra were corrected for the spectral response of the photomultiplier tube used.

Results and discussion

Analysis of the results of weight-loss method

Corrosion rates of mild steel in neutral aqueous environment containing 60ppm chloride in the absence and presence of inhibitor at various concentrations obtained by the weight-loss method are given in Table I. The corrosion inhibition efficiencies of the system, ethyl phosphonic acid (EPA)–Zn^{2+} are also given in Table I.

It is evident from these results that EPA by itself is a poor corrosion inhibitor. Also, Zn^{2+} is found to be corrosive. However, interestingly, EPA–Zn^{2+} combination offers good corrosion inhibition at 300ppm each of EPA and Zn^{2+}. This clearly indicates the synergistic effects of EPA and Zn^{2+} combination. It is observed that the formulation consisting of 300ppm EPA and 300ppm Zn^{2+} offers 88 per cent inhibition efficiency. A thin interference film, embedded in a very thin brown film is observed on the surface of the inhibited metal during the weight-loss experiment.

Table I Corrosion rates of mild steel in neutral aqueous environment (Cl^- = 60 ppm) in the presence and absence of inhibitor and the inhibition efficiencies obtained by the weight-loss method inhibitor system: EPA + Zn^{2+}

S1. No.	Concn. of EPA ppm	Concn. of Zn^{2+} ppm	Corrosion rate mdd	Inhibition efficiency (%)
1	0	0	15.54	–
2	300	0	15.25	2
3	300	10	10.88	30
4	300	50	6.22	60
5	300	100	3.42	78
6	300	150	3.11	80
7	300	200	2.80	82
8	300	300	1.87	88
9	0	300	22.53	–45

Analysis of the uv-visible absorption spectra of solutions

The uv-visible absorption spectra of various test solutions are given in Figure 1. In comparison to the absorbance value at 192nm in the case of 300ppm EPA alone, one can see an increase in the absorbance when 300ppm Zn^{2+} is added to 300ppm EPA. This suggests the possibility of the formation of a complex between EPA and Zn^{2+} in solution. The λmax shifts from 192-235nm, in the case of the solution containing 300ppm EPA and 100ppm Fe^{2+}. Besides, there is an increase in absorbance also. These observations indicate the formation of Fe^{2+}–EPA complex also in solution.

Figure 1 UV-visible absorption spectra of solutions

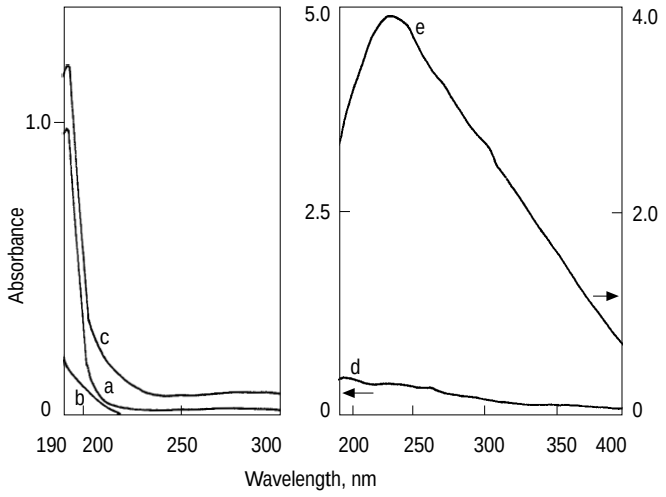

Note: a EPA 300 ppm
b Zn^{2+} 300 ppm
c EPA 300 ppm + Zn^{2+} 300 ppm
d Fe^{2+} 100 ppm
e EPA 300 ppm + Fe^{2+} 100 ppm

Anti-Corrosion Methods and Materials
Volume 45 · Number 5 · 1998 · 338–343

Analysis of the FTIR spectra

The FTIR spectrum of pure EPA is given in Figure 2a. The FTIR spectrum of the film carefully scratched from the surface of the metal immersed in the environment containing 60ppm Cl^- and 300ppm EPA is given in Figure 2b. It is interesting to note that the P-O stretching frequency of EPA decreases from 1,071.1 to 1,025.8cm^{-1}. This shift may be caused by the decrease of electron cloud density of P-O bond. Owing to the shift of the electron cloud density from O atom to Fe^{2+}, it is suggested that the O atom of the phosphonic acid is coordinated to Fe^{2+}[12-17] resulting in the formulation of Fe^{2+}–EPA complex on the metal surface.

The FTIR spectrum of the film scratched from the surface of the metal immersed in the environment consisting of 60ppm Cl^-, 300ppm EPA and 300ppm Zn^{2+} is given in Figure 2c. It is seen from the spectrum that the P-O stretching frequency decreases from 1,071 to 997.5cm^{-1}. This also suggests that the O atom of the phosphonic acid is coordinated to Fe^{2+}. This confirms the formation of Fe^{2+}–EPA complex on the metal surface.

Figure 2 FTIR spectra of EPA (a) and of mild steel surface immersed in various environments (b,c)

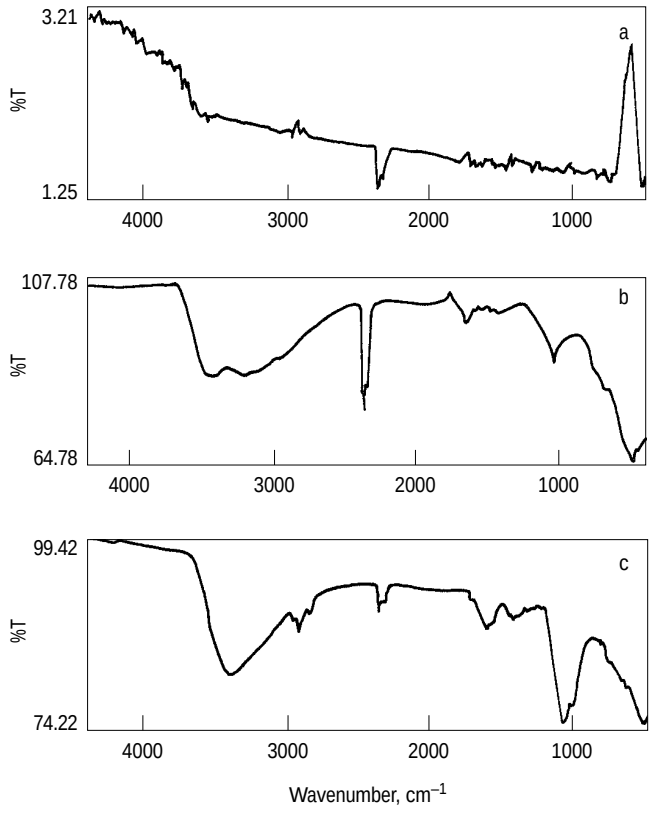

Note: a pure EPA
b $C1^-$ 60 ppm + EPA 300 ppm
c $C1^-$ 60 ppm + EPA 300 ppm + Zn^{2+} 300 ppm

Further, the band at 1,320cm^{-1} is due to Zn(OH)2[1].

Now the following question arises. When the complex formed on the metal surface is the same (i.e. Fe^{2+} – EPA complex), what could be the reason for the observed difference in the corrosion inhibition efficiencies in the presence and absence of Zn^{2+}. The interpretation is as follows. In the absence of Zn^{2+}, the complex formed at the anodic sites is not able to protect the metal surface from corrosion due to the constant action of the aggressive chloride ion which breaks this film on the anodic sites. On the other hand, in the presence of Zn^{2+} and EPA, there is formation of $Zn(OH)^2$ at the cathodic sites which controls the cathodic reaction besides the formation of Fe^{2+} – EPA complex at the anodic sites, and hence, the observed higher corrosion inhibition efficiency in the presence of EPA – Zn^{2+} combination.

Analysis of the uv-visible reflectance spectra

The uv-visible reflectance spectra of the films formed on the surfaces of the metal specimens immersed in various test solutions are given in Figure 3. The uv-visible reflectance spectra of the unpolished metal, of the polished metal immersed in the environment containing 60ppm Cl^-, and that of the polished metal immersed in the environment consisting of 60ppm Cl^- and 300ppm Zn^{2+}, show wavelength transition at 550nm revealing that the band gap (E_g) of the film formed on the above surfaces is E_g = 1.239/0.55 = 2.25 eV. This indicates that the film formed on the above surfaces consists of oxides of iron[18-21] having semiconducting property[22-25].

On the other hand, the uv-visible reflectance spectrum of the polished metal does not show any wavelength transition at 550nm. This may be due to the thinness of the iron oxide film.

The uv-visible reflectance spectrum of the film immersed on the surface of the polished metal immersed in solution containing 60ppm Cl^- and 300ppm EPA (Figure 3e) shows gain wavelength transition at 500nm indicating the presence of oxides of iron. The absorption peak at 235nm corresponds to the presence of Fe^{2+}–EPA complex embedded in oxides of iron.

It is observed from the uv-visible reflectance spectrum of the film formed on the surface of the metal immersed in the

Figure 3 UV-visible reflectance spectra of mild steeel surface immersed in various environments

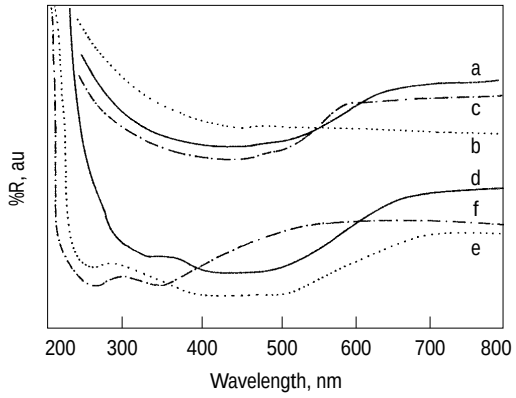

Note: a unpolished
b polished
c polished + $C1^-$ 60 ppm
d $C1^-$ 60 ppm + Zn^{2+} 300 ppm
e $C1^-$ 60 ppm + EPA 300 ppm
f $C1^-$ 60 ppm + EPA 300 ppm + Zn^{2+} 300 ppm

Figure 4 XRD patterns of mild steel surface immersed in various environments

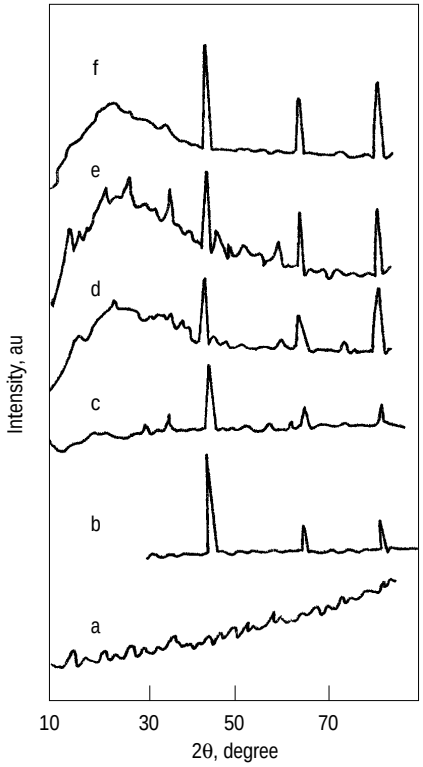

Note: a unpolished
b polished
c polished + $C1^-$ 60 ppm
d $C1^-$ 60 ppm + Zn^{2+} 300 ppm
e $C1^-$ 60 ppm + EPA 300 ppm
f $C1^-$ 60 ppm + EPA 300 ppm + Zn^{2+} 300 ppm

environment consisting of 60ppm Cl–, 300ppm EPA and 300ppm Zn^{2+} (Figure 3f), that wavelength transition takes place at 420nm. The band gap of the protective film is found to be Eg = 1.239/0.42 = 2.95 eV, that is an increase in the value of band gap from 2.25 eV to 2.95 eV upon the addition of 300ppm Zn^{2+} to the formulation consisting of 60ppm Cl– and 300ppm EPA is noticed. It is interesting to note that this protective film offers an inhibition efficiency of 88 percent, as revealed by the weight-loss method. It is also observed from the spectrum that the absorption peak at 240nm corresponds to Fe^{2+}–EPA complex, which is in agreement with the result obtained from the uv-visible absorption spectra of solutions.

Analysis of the X-ray diffraction patterns

The X-ray diffraction (XRD) patterns of the film formed on the surfaces of the metal specimens immersed in various test solutions are given in Figure 4.

The surface of the unpolished metal contains Γ–FeOOH (2θ = 13.6°), Fe_3O_4 (2θ = 35.7°) and α–FeOOH (2θ = 58.2°). The peak due to iron occurs at 2θ = 44.2°[26]. In the case of polished metal, the peaks due to iron appear at 2θ = 44.8°, 65.1°, 82.4° and 99.0°. With the metal specimen immersed in 60ppm Cl– solution, in addition to iron peaks, peaks due to magnetic (Fe_3O_4) occur at 2θ = 30.1°, 35.5° and 62.5°[26]. This indicates that in the chloride environment, mild steel specimen has undergone corrosion leading to the formation of magnetite.

The XRD pattern of the surface of the metal immersed in solution containing 60ppm Cl^- and 300ppm Zn^{2+} is given in Figure 4d. It is observed that the peaks due to iron occur at 2θ = 44.4°, 64.8° and 82.2°. The peaks corresponding to Γ–FeOOH appear at 20 = 36.6° and 61.1°[26].

The XRD pattern of the surface of the metal immersed in the solution containing 60ppm Cl^- and 300ppm EPA is given in Figure 4e. It is found that the brown film formed on the surface contains α–FeOOH (2θ = 52.9°) and Γ–FeOOH (2θ = 14.2°, 36.5°, 47.2° and 60.8°). The peaks due to iron occur at 2θ = 44.9°, 65.3° and 82.6°[26]. The XRD pattern of the surface of the metal immersed in the solution containing 60ppm Cl^-, 300ppm EPA and 300ppm Zn^{2+} is given in Figure 4f. It is observed that the peaks due to iron occur at 2θ = 44.9°, 65.2° and 82.6°. The peaks due to oxides of iron such as Fe_3O_4, a–FeOOH and Γ–FeOOH are found

Anti-Corrosion Methods and Materials
Volume 45 · Number 5 · 1998 · 338–343

to be absent, even though visual observation reveals very small amount of brown film along with a thin interference film. It may be due to the fact that this film is too thin to be detected by XRD technique.

Analysis of the luminescence spectra

The luminescence spectra (λ_{ex} = 300nm) of the films formed on the surfaces of the metal specimens immersed in various test solutions are given in Figures 5a and 5b. The luminescence spectrum of the film formed on the surface of the metal immersed in 60ppm Cl^- and 300ppm EPA is given in Figure 5a. It is observed that the intensities of the peaks are very weak. However, increase in intensities of the peaks is noticed in the presence of 60ppm Cl^-, 300ppm EPA and 300ppm Zn^{2+}. This can be explained as follows. Ethyl phosphonic acid alone is not a good inhibitor, and there is formation of several oxides of iron on the surface. The composition of these oxides is so high that the complex formed between Fe^{2+} and EPA is masked, and hence, decrease in intensity of the luminescence. In the presence of EPA and Zn^{2+}, 88 per cent inhibition efficiency is achieved because of the enhanced formation of the protective film of Fe^{2+}–EPA complex. This film is not very much masked by oxides of iron, and hence, increase in intensity of the luminescence is noticed.

Mechanism of corrosion inhibition

Results of the weight-loss method reveal that the formulation consisting of 300ppm ethyl phosphonic acid (EPA) and 300ppm Zn^{2+} offers an inhibition efficiency of 88 per cent. The uv-visible absorption spectra indicate the possibility of formation of the Fe^{2+}–EPA complex and also Zn^{2+}–EPA complex in solution. The FTIR spectra show that Fe^{2+}–EPA complex and $Zn(OH)_2$ are present on the inhibited metal surface. Luminescence spectra reveal that the formation of Fe^{2+}–EPA complex on the metal surface is enhanced by the presence of Zn^{2+} in the environment. The uv-visible reflectance spectra show the presence of Fe^{2+}–EPA complex on the metal surface and the band gap of the protective film is found to be 2.95eV. The XRD pattern of the protective film corresponds to iron peaks only. In order to explain all the observations in a holistic way, a suitable mechanism of corrosion inhibition is proposed as follows:

(1) When mild steel specimen is immersed in the neutral aqueous environment, the anodic reaction is:
$Fe \rightarrow Fe^{2+} + 2e^-$
And the cathodic reaction is:
$2\ H_2O + O_2 + 4e^- \rightarrow 4\ OH^-$

(2) When the environment consisting of 60ppm Cl^- + 300ppm EPA + 300ppm Zn^{2+} is prepared, there is formation of Zn^{2+}–EPA complex in solution.

(3) Now, when the metal (mild steel) is immersed in this environment, the Zn^{2+}–EPA complex diffuses from the bulk of the solution to the surface of the metal.

(4) On the surface of the metal, Zn^{2+}–EPA complex is converted into Fe^{2+}–EPA complex in the local anodic regions as the latter is more stable than the former:
Zn^{2+}–EPA + $Fe^{2+} \rightarrow Fe^{2+}$–EPA + Zn^{2+}
(This reaction takes place on the surface of the metal in the local anodic regions.)
(Formation of Fe^{2+}–EPA complex also to some extent cannot be ruled out.)

(5) Now, the released Zn^{2+} ion on the surface will form $Zn(OH)_2$ precipitate in the local cathodic regions:
$Zn^{+2} + 2\ OH^- \rightarrow Zn(OH)_2$

(6) Thus, the protective film consists of Fe^{2+}–EPA complex, $Zn(OH)_2$ and very thin film of oxides of iron.

Figure 5 Luminescence spectra of mild steel surface immersed in various environments

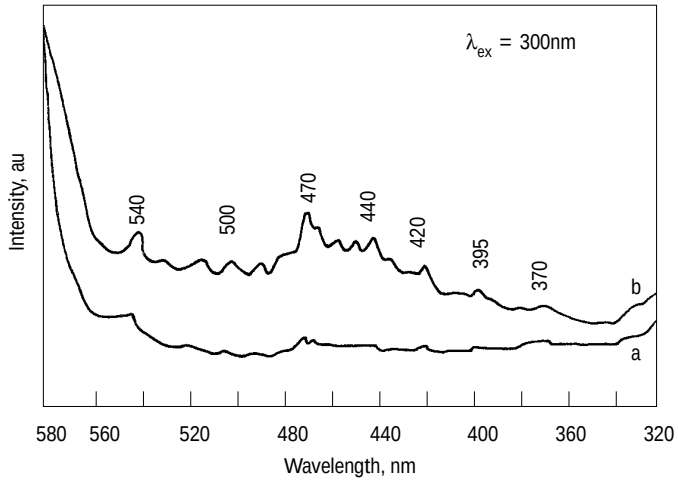

Note: a C1⁻ 60 ppm + EPA 300 ppm
b C1⁻ 60 ppm + EPA 300 ppm + Z^{2+} 300 ppm

Conclusions

(1) The formulation consisting of 300ppm EPA and 300ppm Zn^{2+} has 88 per cent inhibition efficiency.

(2) The protective film formed on the metal surface is found to be luminescent and to consist of Fe^{2+}–EPA complex, $Zn(OH)_2$ and a very thin film of oxides of iron.

References

1 Sekine, I. and Kirakawa, Y., *Corrosion,* Vol. 42, 1986, p. 276.

2 Fang, J.L., Li, Y., Ye, X.R., Wang, Z.W. and Liu, Q., *Corrosion*, Vol. 49, 1993, p. 266.

3 Mathiyarasu, J., Natarajan, R., Palaniswamy, N. and Rengaswamy, N.S., *Bulletin of Electrochem*, Vol. 13, 1997, p. 161.

4 Gunasekaran, G., Palaniswamy, N., Apparao, B.V. and Muralidharan, V.S., *Electrochem Acta*, Vol. 49, 1997, p. 1427.

5 Rajendran, S., Apparao, B.V. and Palaniswamy, N., *Proc. 8th Europ. Symp. Corros. Inhibitors,* Ferrara, Italy, Vol. 1, 1995, p. 465.

6 Rajendran, S., Apparao, B.V. and Palaniswamy, N., *Bulletin of Electrochem*, Vol. 12, 1996, p. 15.

7 Rajendran, S., Apprarao, B.V. and Palaniswamy, N., *Proc. 2nd Arabian Corrosion Conference*, Kuwait, 1996, p. 483.

8 Rajendran, S., Apparao, B.V. and Palaniswamy, N., *EUROCORR '97*, Trondheim, Norway.

9 Rajendran, S., Apparao, B.V. and Palaniswamy, N., *Anti-Corrosion Methods and Materials,* September/ October, 1997.

10 Hatch, G.B. and Ralston, P.H., *Mat. Pro. Perf.*, Vol. 11, 1972, p. 39.

11 Rajendran, S., Apparao, B.V. and Palaniswamy, N., The 10th Asia Pacific Corrosion Control Conference, Bali, Indonesia, 27-31 October 1997.

12 Silverstein, R.M., Bassler, G.C. and Morrill, T.C., *Spectrometric Identification of Organic Compounds,* John Wiley and Sons, New York, NY, 1981, p. 95.

13 Nakamoto, K., *Infrared and Raman Spectra of Inorganic and Coordination Compounds,* Wiley-Interscience, New York, NY, 1986, p. 168.

14 Cross, A.D., *Introduction to Practical Infra-red Spectroscopy*, Butterworths Scientific Publication, London, 1960, p. 73.

15 Smith, T.D.J., *Inorg. Nucl. Chem.,* Vol. 9, 1959, p. 150.

16 Horner, L. and Horner, C.L., *Werkst. Korros.*, Vol. 27, 1976, p. 223.

17 Bohnsack, G., *UGB Kraftwerkstechnik,* Vol. 66, 1986, p. 48.

18 Sharon, M., Tamizhmani, G. and Basaraswaram, K., *Proc. Indian Nat. Sci. Acd.*, Vol. 52, 1986, p. 311.

19 Sanchez, H.L., Steinfink, H. and White, H.S., *J. Solid State Chem.*, Vol. 41, 1982, p. 90.

20 Sharon, M. and Prasad, B.M., *Solar Energy Mat.,* Vol. 8, 1983, p. 457.

21 Sanchez, C., Sieber, K.D. and Somorjai, G.A., J. *Electroanal, Chem.*, Vol. 252, 1988, p. 269.

22 Schultze, W. and Stimming, U., *Z. Phys. Chem. N.F.,* Vol. 98, 1975, p. 285.

23 Wilhelm, S.M., Yun, K.S., Ballenger, L.W. and Hackerman, N., *J. Electrochem. Soc.*, Vol. 126, 1979, p. 416.

24 Wilhelm, S.M. and Hackerman, N., *J. Electrochem. Soc.*, Vol. 128, 1981, p. 1668.

25 Abrantes, L.M. and Peter, L.M., *J. Electroanal. Chem.,* Vol. 150, 1983, p. 593.

26 Favre, M. and Landolt, D., *Corrosion Science*, Vol. 34, 1993, p. 1481.